EXAMINING URBAN EXPANSION IN THE GREATER TORONTO AREA USING LANDSAT IMAGERY FROM 1974–2014

Lanying Wang, Wei Li, Shiqian Wang, and Jonathan Li
GeoSTARS Lab, Department of Geography & Environmental Management,
University of Waterloo, Ontario, Canada

The Greater Toronto Area is the most vital economic centre in Canada and has experienced rapid urban expansion in the past 40 years. This research uses Landsat images to detect the spatial and temporal dynamics of urban expansion in the Greater Toronto Area from 1974 to 2014. We quantitatively analyzed the extent of urban expansion and spatial patterns of growth from classified Landsat images. We then integrated our expansion findings with population data to observe the relationships between urban growth and population. We found that the Greater Toronto Area had significant growth of 1115 km², expanding mainly in radiated and ribbon expansion modes. There was substantial correlation between urban extent and population in the period of study. These results demonstrate the efficacy of combining statistical population data with remote sensing imagery for the analysis of urban expansion.

La région du Grand Toronto est le centre économique le plus important au Canada et a connu une expansion urbaine accélérée au cours des 40 dernières années. Cette recherche utilise des images Landsat pour détecter les dynamiques spatiale et temporelle de l'expansion urbaine de la région du Grand Toronto entre 1974 et 2014. Nous avons analysé, sur le plan quantitatif, l'expansion urbaine et les tendances spatiales de croissance à partir des images Landsat classifiées. Ensuite, nous avons intégré nos résultats aux données de population afin d'observer les liens entre la croissance urbaine et la population. Nous avons déterminé que la région du Grand Toronto avait connu une importante croissance de 1 115 km² de même qu'une expansion principalement dans les modes en rayonnement et en ruban. Il y a eu une importante corrélation entre l'étendue urbaine et la population pendant la période étudiée. Ces résultats démontrent à quel point il est efficace de combiner les données statistiques de population et les images de télédétection pour analyser l'expansion urbaine.

Lanying Wang
L333wang@uwaterloo.ca

Wei Li
w257li@uwaterloo.ca

Shiqian Wang
s358wang@uwaterloo.ca

Jonathan Li
junli@uwaterloo.ca

1. Introduction

Urbanization represents the absorption of less developed areas, such as agricultural and forest land, by built-up areas, such as residential and commercial land. Some researchers suggest that urban expansion is an indicator of a region's economic vitality [*Yuan et al*. 2005]. Urban expansion is typically a product of the development of suburban areas into high-density built-up areas and the replacement of rural areas with low-density built-up areas. Urban expansion not only affects the economics in the region, but also influences ecosystem balances, as reflected in changes in water quality and receding agricultural and forest areas [*Squires* 2002]. As a result, studies of urban expansion are quite important for local or regional planners, as well as policy makers in helping them to make reasonable and effective decisions for planning, environmental management, and land resources integration [*Yuan et al*. 2005; *Dewan and Yamaguchi* 2009].

Decision-makers require the latest geographical information on urban sprawl patterns in both quantitative and qualitative ways; therefore, it is important to keep geospatial information of urban expansion up to date. In recent years, remotely-sensed images have become a great data source for urban expansion research. There are an increasing number of studies that focus on using remote sensing technology to monitor urban dynamic changes. Some studies have shown that remote sensing can provide an accurate measure of land use and land cover (LULC) changes, which are

dx.doi.org/10.5623/cig2015-203

able to represent urban expansion, especially at medium scales [*Yuan et al*. 2005; *Schneider* 2012; *Bagan and Yamagata* 2012]. Compared to traditional LULC monitoring methods, such as field surveys, remote sensing offers a more efficient, cost -effective, and less labor-intensive technique in detecting LULC changes. Mapping LULC changes at various spatial and temporal scales is facilitated using remote sensing techniques [*Elvidge et al*. 2004]. For instance, at small scales, the Moderate Imaging Spectroradiometer (MODIS) sensors can provide daily image products at 250 m and 500 m spatial resolution, and the Advanced Very High Resolution Radiometer (AVHRR) sensors can supply 1.1 km resolution images every 12 hours. Since the first Landsat satellite was launched in 1972 (initially as ERTS-1), the Landsat series of satellites have been collecting multi-spectral data at 80 m (1972–1982) and 30 m (1982–present) spatial resolution and at 16 or 18 days temporal resolution. Since they are easily accessible through the United States Geological Survey (USGS) Landsat Data Archive, and have relatively high spatial resolution and long historical data archive, Landsat images have been commonly used to detect LULC changes at different scales [*Manandhar et al*. 2009]. Images of Landsat Multispectral Scanner (MSS), Landsat Thematic Mapper (TM), Landsat-7 Enhanced Thematic Mapper Plus (ETM+), and Landsat-8 Operational Land Imager (OLI), were used in this study for collecting LULC change information for the study area.

Change detection is "the process of identifying differences in the state of an object or phenomenon by observing it at different times" [*Singh* 1989]. Change detection methods that have been used for analyzing dynamic LULC changes include Principal Component Analysis, Write Function Memory, and Change Vector Analysis [*Singh* 1989]. All these methods can be classified into pre-classification and post-classification techniques [*Yuan et al*. 1998], wherein the pre-classification methods produce change/non-change maps. Although they are effective at documenting overall change, they cannot demonstrate the nature of the information change [*Singh* 1989]. The post-classification algorithm requires the user to classify images before generating the "from-to" change maps. Although the accuracy of post-classification change detection methods rely heavily on the accuracy of classification results, thematic maps and valuable "from-to" change maps can be generated by the whole procedure of the post-classification method [*Fu* 2014]. As a result, many studies focusing on LULC change and urban expansion apply post-classification comparison change detection methods to identify specific categories of LULC, and thus explore the change pattern and change effect on the surrounding environment [*Abd El-Kawy et al*. 2011; *Yuan et al*. 2005; *Sundarakumar et al*. 2012; *Peiman* 2011; *Tan et al*. 2010].

In this study, the post-classification comparison change detection approach was used, necessitating the selection of an appropriate classification algorithm. Since unsupervised classifiers need a large amount of work during the post-classification period, various supervised classification methods have been developed, such as Minimum Distance [*Wacker and Landgrebe* 1972], Maximum Likelihood (MLC) [*Otukei and Blaschke* 2010], and Artificial Neural Network (ANN) [*Erbek et al*. 2004]. Compared with traditional statistical classifiers (e.g. MLC), the Support Vector Machine (SVM) classifier is a different type of classification algorithm. SVM is a method based on the statistical learning theory and the structural risk minimization method and has had an excellent track record of image classification [*Schneider* 2012; *Huang et al*. 2002; *Yang* 2011]. Based on the previous studies, the SVM, MLC, and ANN classifiers were tested, and their relative performances were evaluated.

Satellite-based LULC changes in the Greater Toronto Area (GTA) have been the focus of several previous studies. For example, *Martin and Howarth* [1989] used SPOT multispectral imagery to detect the landscape's change in the City of Scarborough, a small part of the GTA. An object-oriented classification of IKONOS images of the City of Mississauga within the GTA, was reported by *Lackner and Conway* in 2008. *Ferrato and Forsythe* [2013] compared classification results from Earth Observing-1 Hyperion hyperspectral data with Landsat and SPOT data through iterative self-organizing data analysis. Although they validated the relative information content of each of the satellite data sources, they only used one year for classifying the land use, thereby limiting their ability to provide a dynamic change analysis of the study area. *Hu and Ban* [2008] used Landsat and RADARSAT images to monitor urban changes in the GTA between 1988 and 2002. Similarly, *Li and Zhao* [2003] presented a bi-temporal change detection study using Landsat TM images, which only focused on the City of Mississauga. Though they were able to successfully show changes, their study only identified "from-to" changes based on two

years and they only applied a single classifier in their classification process. *Forsythe* [2002], *Furberg and Ban* [2008], and *Tole* [2008] proposed the use of multiple Landsat images to monitor urban sprawl. *Conway and Hackworth* [2007] used the Normalized Difference Vegetation Index (NDVI) to detect the urban land cover variation through Landsat images in the GTA with an over 90% overall classification accuracy. However, only two or three images were used to represent the urban expansion trend of decades. Overall, most of these studies used few images and only one classification algorithm to carry out an assessment of long period dynamic change that did not cover the entire GTA.

This research expands on these studies by examining the dynamic changes in the processes of urban expansion of the GTA over a period of 40 years. We applied multiple classification methods and evaluated LULC changes of bi-temporally (i.e. between years) and multi-temporally (i.e. across all years) from Landsat data sets at 5-year intervals from 1974 to 2014. Our study focused on the quantitative and qualitative analysis of regional urban expansion. Another objective of the study was to analyze the relationship between population and urban expansion. Population as one of the driving factors for urban expansion analysis has been playing an important role of urban development monitoring. *Ma and Xu* [2010] pointed out that population growth would lead to increased demand by urban residents on land resources and urban space such as residence ad traffic and public facilities. *Silván-Cárdenas* [2010] used fine spatial resolution images for population estimation in small areas and proposed that population estimation using remotely-sensed images is receiving more attention. Thus, we examine the relationship between population and urban expansion over the last 40 years.

2. Study Area and Data

2.1 Study Area

The study area (see Figure 1) is located in Southern Ontario, Canada, including the City of Toronto, and Regions of Durham, Halton, Peel, and York [*Statistics Canada* 2011]. This area covers 7752 km^2, and is located between Lake Ontario and Georgian Bay of Lake Huron. The GTA is the economic centre of Canada and is an important metropolitan area for foreign investment, trade flows, and a hub for exchanges of culture, religion, and technology. It is also the biggest city in Canada due to a large net migration involving immigration, non-permanent residents, interprovincial and intra-provincial migration that has occurred over the past several decades. This study area includes various types of land cover types: lakes and rivers, high and low density urban areas, and rural area (agriculture land, forest landscapes, grassland). According to *Statistics Canada* [1976; 2011], the population of the GTA in 2011 was 6 054 191, a 90% increase from 1976.

2.1 Data Description

Images from the Landsat-1 and -2 Multispectral Scanner (MSS), Landsat-5 Thematic Mapper (TM), Landsat-7 Enhanced Thematic Mapper Plus (ETM+), and Landsat-8 Operational Land Imager (OLI) were the main data sets used in this study (Table 1). All these images were acquired from the Landsat Data Archive held by the USGS, and most were cloud free. We obtained these images in level-one product format. In order to obtain high-quality results of analysis, most of these data were acquired in the summer season from June to September. All images were projected in the World Geodetic System of 1984 (WGS84) and Universal Transverse Mercator (UTM) coordinates. Image pre-processing was performed using the software Environment for Visualizing Images (ENVI) version 4.8, PCI Geomatica 2013, and ArcMap version 10.1. During the image pre-processing, layer stacking for each image was performed first, followed by overlapping images registration. The PCI Geomatica ATCOR module was used to carry out atmospheric correction for each image, based on unique features of data acquisition, including date and time, sensor type, coordinates of the image centre, atmospheric definition area, and atmospheric condition. Finally, images from each year were mosaicked by georeferenced based mosaicking tool in ENVI, with colour balance using and clipped to the bounds of the study area. The GTA boundary and region's boundaries were provided by *Statistics Canada* [2011], and the Lake Ontario boundary acquired for *DMTI Spatial Inc., Ontario* [2014].

Population changes over the last four decades were used to foster an understanding of the urbanization process of the GTA, dating back to 1976 [*Statistics Canada* 2011]. The population data of the GTA were acquired from Statistics Canada from 1976 to 2011 at 5-year intervals [*Statistics Canada* 2011]. The data were then used to analyze the relationship between the population and urban

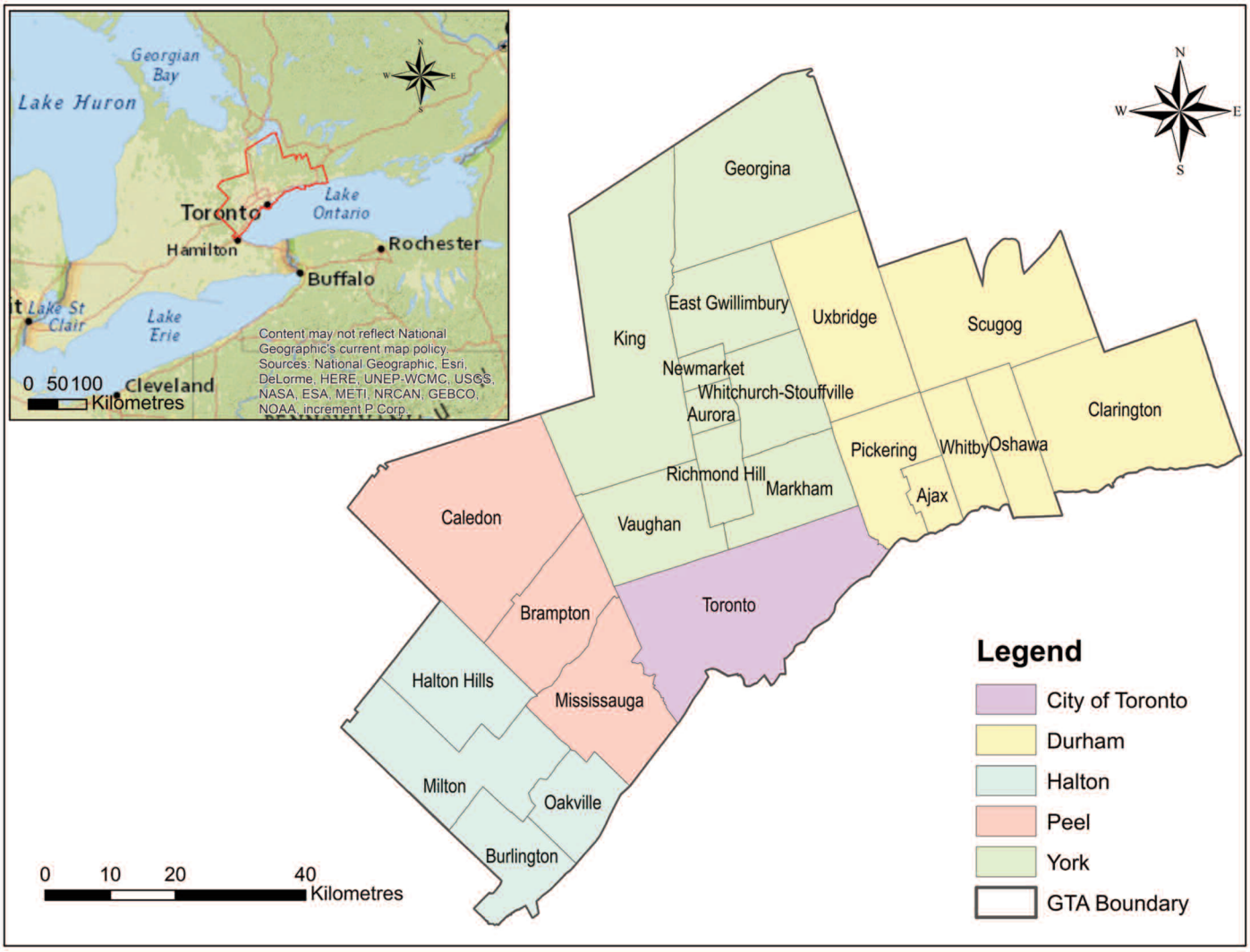

Inset map sources: National Geographic, Esri, DeLorme, HERE, UNEP-WCMC, USGS, NASA, ESA, METI, NRCAN, GEBCO, NOAA, increment P Corp.

Figure 1: Study area – the Greater Toronto Area (GTA).

Table 1: Satellite images with 5-year intervals used in this study.

Year	Day of the year	Sensor	Bands	Pixel Size
1974	187, 223, 240	MSS	4, 5, 6, 7	60 m
1979	170, 171	MSS	4, 5, 6, 7	60 m
1984	237, 238	TM	1, 2, 3, 4, 5, 7	30m
1989	203, 233	TM	1, 2, 3, 4, 5, 7	30m
1994	174, 178, 185	TM	1, 2, 3, 4, 5, 7	30m
1999	246, 271	ETM+	1, 2, 3, 4, 5, 7	30m
2004	172, 179	TM	1, 2, 3, 4, 5, 7	30m
2009	178, 217	TM	1, 2, 3, 4, 5, 7	30m
2014	192, 199	OLI	1, 2, 3, 4, 5, 6, 7, 9	30m

expansion. A set of full-colour 10–20 cm resolution digital orthoimages in 2009 were acquired from the Geospatial Centre, University of Waterloo as a reference map for accuracy assessment in 2009.

3. Methods

The analysis methods can be divided into three parts: image classification, change detection and analysis, and urban expansion analysis as shown in Figure 2. All image processing was performed using ENVI 4.8 and ArcMap 10.1.

3.1. Image Classification

Selecting an appropriate algorithm to classify the imagery during the initial stages of this analysis was vital, as the quality of the classified images directly impacted the performance of the change detection. To generate consistent classification results, an appropriate classification method was determined first. In this paper, the supervised MLC, SVM, and ANN algorithms were applied to the 2009 mosaic. Training samples were selected for the six Level-2 classes in the classification scheme listed in Table 2. A false colour combination (near infrared band as red, red band as green, and green band as blue) of the reflective spectral band dataset for 2009 was used to choose training samples for those three classification algorithms. A Jeffries-Matusita (JM) distance report was automatically generated to illustrate the spectral separability of the training samples. JM distance is a separability function that detects the average distance between a pair of classes that directly relates to the probability of how accurate a resultant classification will be [*Schmidt and Skidmore* 2003]. Values range from 0 to 2, and the value is asymptotic to 2, meaning that the training samples selected are more separable. After applying classification algorithms, a 3 x 3 majority filter was applied in order to remove the salt-and-pepper noise, as a larger size filter would decrease the accuracy of the final results.

After classification, a statistical accuracy assessment was built to assess the accuracy of classification maps. In order to reduce the cost and time, and to ensure it is large enough to generate an appropriate error matrix, a general guideline to collect sample size is a minimum of 50 samples for each class [*Congalton and Green* 1999]. Based on the 2009 orthoimagery, 600 pixels (100 samples for each Level-2 category) were randomly selected from the classified image of 2009. Selected pixels

Table 2: Image classification categories.

Level-1 category	Level-2 category	Description
Urban area	Residential	Low-density built-up areas, e.g. houses
	Commercial	High-density built-up areas, e.g. commercial areas and parking lots
Non-urban area	Barren Cropland	Fallow / harvested agriculture areas
	Water-body	River, lake, and pond areas
	Forest	Forest cover areas
	Vegetation	Grassland, parks, and agricultural area in production

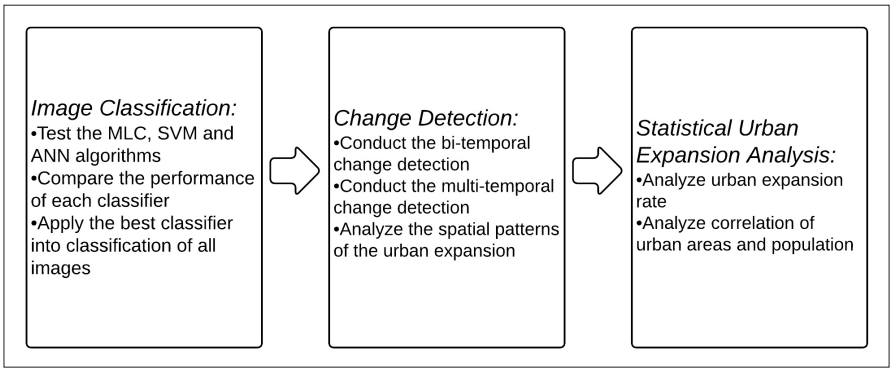

Figure 2: The workflow chart of this study.

were manually validated against the orthoimagery. The overall accuracy, the user's accuracy (the probability that a classified pixel is really in that category) and the producer's accuracy (the probability an area is correctly classified) were calculated through the error matrix [*Congalton* 1991]. An advanced measure of interclass agreement, the Kappa coefficient, was also calculated. The Kappa coefficient provides a better interclass discrimination than the overall accuracy statistic alone [*Fitzgerald and Lee* 1994].

3.2 Change Detection

In the change detection analysis process, the post-classification comparison change detection method was applied to detect land use and land cover changes. Post-classification comparison separately classifies multi-temporal images into thematic maps, and then implements a comparison of the classified images on a per-pixel basis [*Alphan et al*. 2009]. This approach can produce change maps that show a complete matrix of changes by properly coding the classification results of two dates. Before applying the change detection, the LULC classes were combined into Level-1 categories (as shown in Table 2): the urban area and the non-urban area, since we only wanted to examine which area was developed into urban area (the built-up area), and this step can help decrease the impact of classification errors. Bi-temporal and multi-temporal change maps were generated to analyze the spatial patterns of the urban expansion.

Table 3: Accuracy assessment comparison between different classifiers for the 2009 imagery.

	MLC		ANN		SVM	
Level-2 category	UA	PA	UA	PA	UA	PA
Vegetation	0.88	0.95	0.86	0.99	0.90	0.97
Residential	0.90	1.00	0.95	0.95	0.93	0.97
Commercial	0.85	0.83	0.95	0.83	0.93	0.90
Barren Cropland	0.91	0.78	0.93	0.70	0.96	0.83
Water-body	1.00	0.97	1.00	1.00	1.00	1.00
Forest	0.98	0.91	0.98	0.90	0.94	0.88
Cloud	0.50	1.00	1.00	0.50	1.00	0.33
Shadow	0.60	1.00	0.50	1.00	1.00	1.00
Overall accuracy (%)	85.34		91.48		92.63	
Kappa coefficient	0.83		0.89		0.90	
(UA = user's accuracy; PA = producer's accuracy)						

3.3 Statistical Urban Expansion Analysis

Both the rate and spatial structure of urban expansion vary across time [*Bagan and Yamagata* 2012]. We calculated the rate of urban expansion using the Land Use Change Index (LUCI), as shown in equation (1) [*Haregeweyn* 2012]. This has been shown to be a significant index for assessing urban expansion [*Bagan and Yamagata* 2012].

$$LUCI = \frac{(U_a - U_b)}{T \times U_b} \times 100, \quad (1)$$

where Ua and Ub indicate the area of a land use class at Time a and Time b, respectively. T indicates the time period from Time a to Time b. If T's unit is in years, then LUCI will be the annual rate of change in the area for this class. In our case, the LULC class was the overall urban class. At the same time, we carried out a Pearson correlation coefficient analysis to analyze the correlations between the urban areas and the population.

4. Results and Discussion

4.1 Classification Accuracy

An error matrix was built to assess the accuracy of the classification results before choosing an appropriate classifier across all time periods. As shown in Table 3, the overall accuracy of the SVM classifier was 92.63%, and the Kappa coefficient was 0.90. In comparison, the MLC algorithm had an overall accuracy of 85.34%, with a Kappa coefficient of 0.83, and the ANN algorithm had an overall accuracy of 91.48%, with a Kappa coefficient of 0.89. Both the MLC algorithm and ANN algorithm were inferior compared to the SVM. The user's and producer's accuracies of commercial areas and barren cropland in SVM were much better than the results from the ANN and MLC. Therefore, we proceeded to classify the remaining images from the other years with the SVM classifier. During the classification process, we combined the Level 2 categories together into either urban area or non-urban areas. This process reduced misclassification.

4.2 Map Changes and Analysis

By counting the number of pixels of each image, the bi-temporal change detection results indicated an increase in the GTA's urban area of 1115 km² (from 1122 km² in 1974 to 2237 km² in 2014, as shown in Figure 3). By extracting and overlaying the urban area of the multitemporal classification results, the urban expansion map was compiled, including 10-year intervals from 1974 to 2014 (Figure 4). Based on Figures 3 and 4, some important spatial patterns could be observed. The spatial urban expansion in the GTA mainly followed two types: radiated expansion mode, which is a typical tendency of urban growth that from urban centres to adjoining non-urban areas by a series of concentric circles [*Burgess* 2008]; ribbon expansion mode, which is a combination type of border [*Stan* 2013] and enclave [*Stan* 2013] types, which the growth was starting with, several centres along the lakeshore of Lake Ontario.

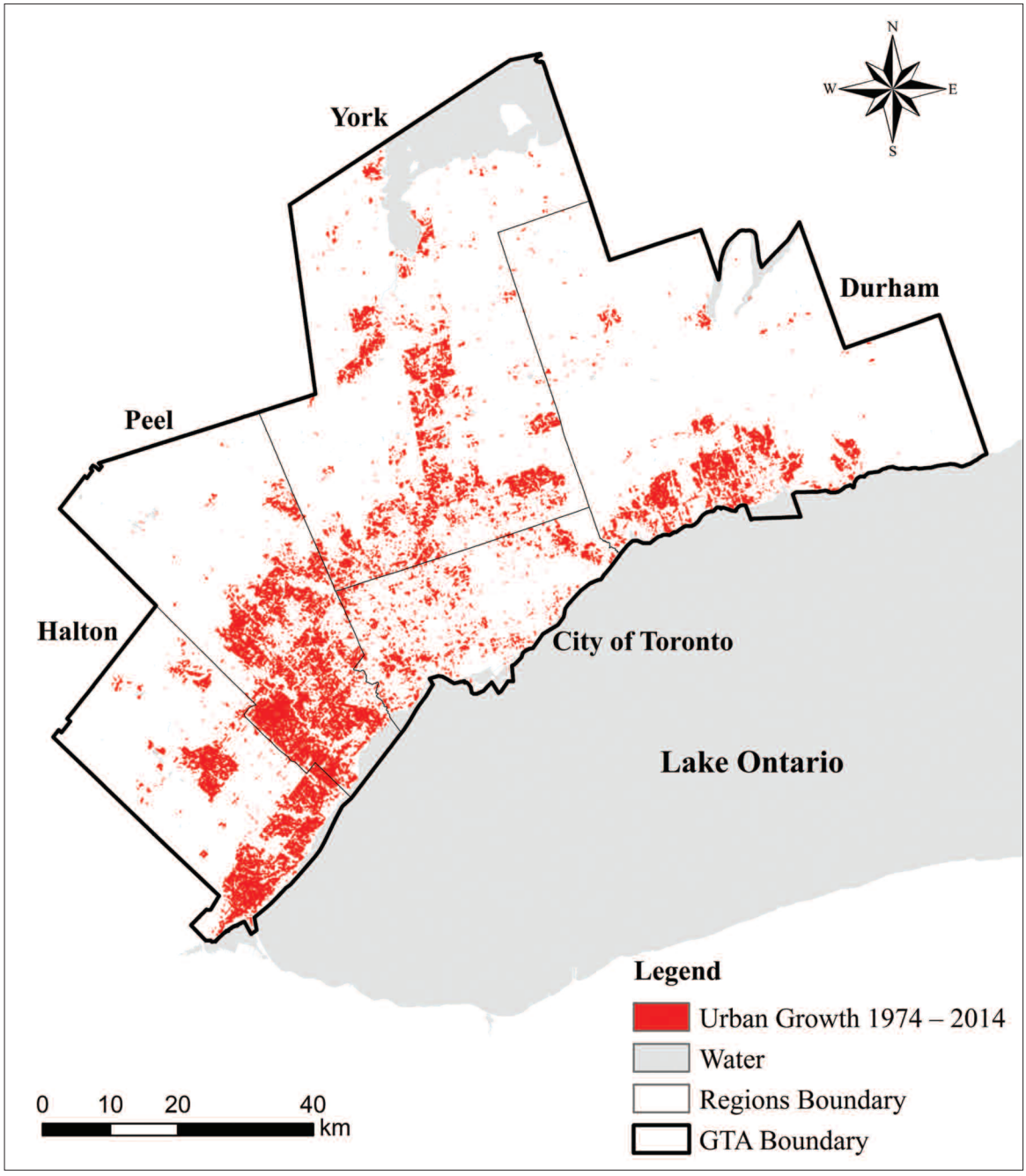

Figure 3: The bi-temporal change detection from 1974 to 2014.

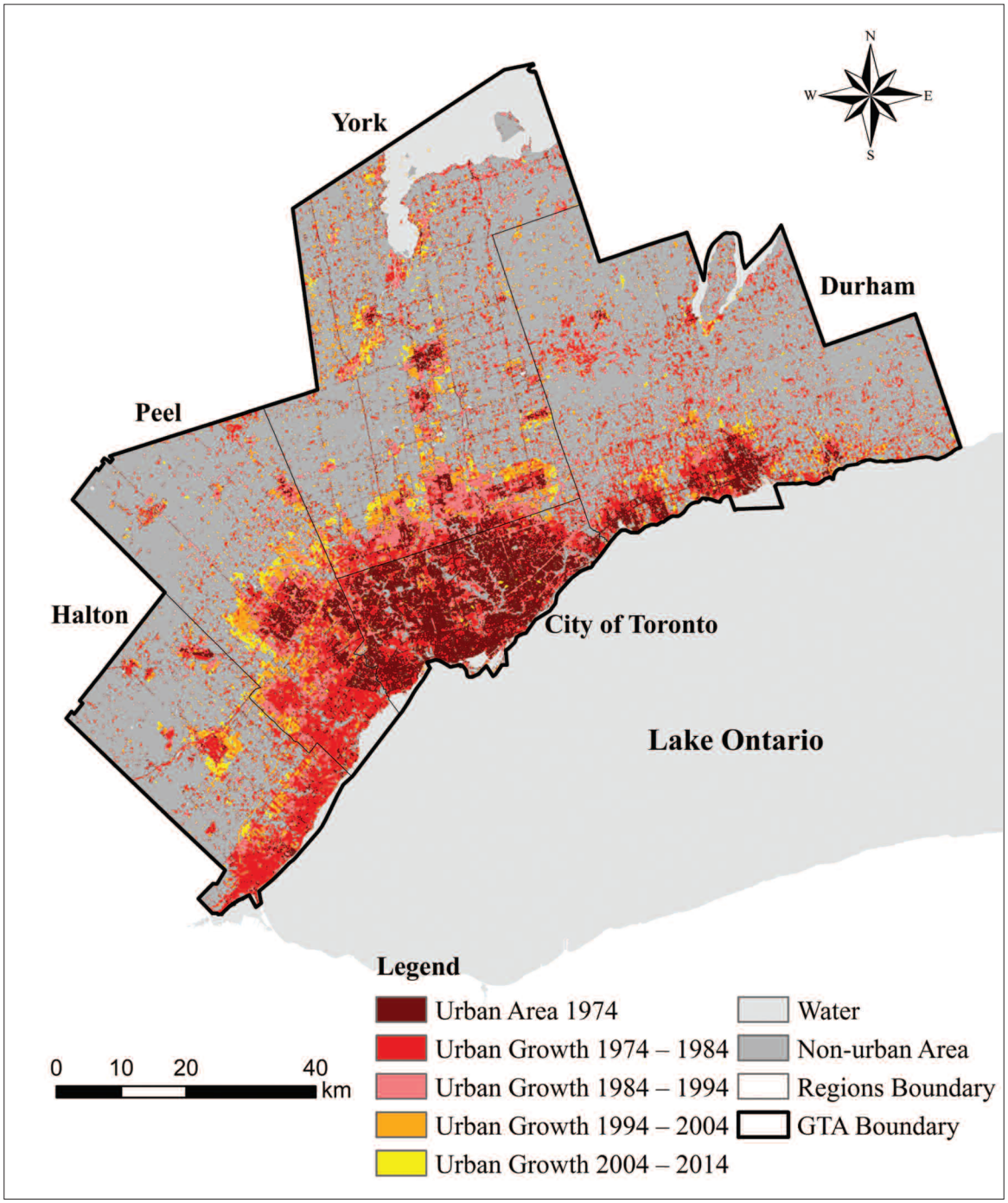

Figure 4: The multi-temporal change detection from 1974 to 2014.

Table 4: Annual growth rate of the urban area between 1974 and 2014.

	1974–1979	1979–1984	1984–1989	1989–1994	1994–1999	1999–2004	2004–2009	2009–2014
Annual growth rate (%)	-1.1	2.2	4.3	1.9	0.7	3.6	0.1	1.4
Mean annual growth rate (%) = 1.6								

The GTA expanded outward from the City of Toronto, as well as laterally along Lake Ontario's lakeshore. In addition, regional centres of Peel, Durham, and York also expanded. In 1974, many of the regional centres within the GTA existed in isolation, as shown in Figure 4, and the cities could be clearly identified individually. From 1974 to 1991, regions around the City of Toronto witnessed a significant growth along their boundaries with Toronto. In the 1990's, the regions of Peel, York, and Durham developed rapidly. All these regions expanded outward from their regional centres. After 2004, York Region's urban expansion began to slow down, while the outside regions (Durham, Peel and Halton) had a considerable growth of urban areas. From 2009 to 2014, the largest expansion occurred in the southwest part of the GTA. For instance, Brampton expanded northeast toward the City of Vaughan. After 40 years of development, some smaller urban centres had connected with each other, such as Richmond Hill and Markham. Furthermore, some cities located along Lake Ontario, such as Burlington, Oakville, and Ajax, experienced significant development. Regions of Peel and Halton had the largest increase in urban area in the GTA. Overall, the urban development in the GTA takes the form of outward extension and expansion from these urban centres, especially from the City of Toronto.

4.3 Statistical Analysis of Urban Expansion and Population

To explore the long-term population and urban growth of the GTA, we calculated the urbanized extent for each 5-year period from our classified imagery and graphed them with population data (Figure 5). As seen on this chart, both population and urban areas experienced constant growth in this time period. Correlation analysis shows that urban expansion is directly correlated to population increase. The Pearson correlation coefficient (r) between the population and the urban area was 0.979 ($p<0.01$), which identifies strong correlation between the population and the urban area in the GTA.

The mean annual growth rate of the urban area over the 40 years was 1.6% (Table 4). There was significant urban expansion during two periods. The periods between 1984–1989 and 1999–2004 saw increases of 4.3% and 3.6% in annual growth rate of the urban area, respectively. A slightly negative trend of 1.1% in 1974–1979 may have been the result of misclassification, as these images were acquired by Landsat-1 at 60 metres pixel size and only 4 bands were available for the classification process. The period between 2004 and 2009 had a lower annual growth rate of 0.1%. This may be due to two main factors: the low urban growth rate in 2004–2009 and the lower classification accuracy of the 2004 image.

According to *Bhatta* [2010], urban expansion can be caused by a variety of reasons such as population growth, economic growth, independence of decision, industrialisation and etc. As *Stan* [2013] pointed out, the three main forces that result in urban expansion are "a growing population, rising incomes, and falling commuting costs." Thus, when we explored deeper into the population changes during these 40 years, we discovered that the two significant periods of urban growth mirrored the population growth over the same time. The mean annual population growth rate over the 40 years was 1.9%, however during the two 5 year periods between 1986–1991 and 1996–2001, more substantial increases were observed of 2.6% and 2.0% were observed respectively. From 1976 to 2011, the annual population growth rate ranged between 1.5% and 2.6%. The lowest annual population growth rate was found in the period of 1976–1981 at 1.5%. It is obvious that urban expansion is typically delayed by a few years following a large increase in population, as the city requires time to respond. The fluctuations in the annual growth rate of the urban area and the annual population growth rate were relatively consistent.

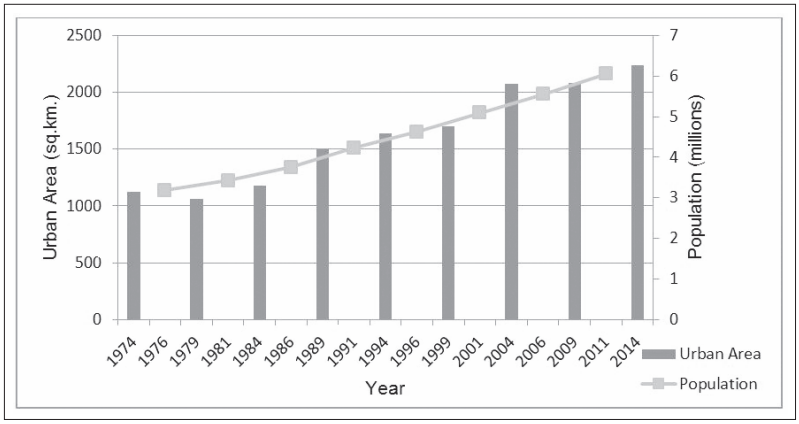

Figure 5: Population growth and urbanization in the GTA from 1974 to 2014.

5. Conclusion

In this paper, dynamic changes of the urban growth trend of the GTA were successfully detected using a series Landsat images acquired over time. The selection of an accurate classification process

was an important part of this study, as it determined the reliability of the final change detection results. In our tests, we found that the SVM classification method performed better than the MLC and ANN approaches. We noted that urban growth occurred mainly in a radiated expansion mode, in which the city expanded outward from the City of Toronto. The GTA also expanded in a ribbon expansion mode along Lake Ontario. Furthermore, the urban expansion was strongly correlated to increases in population. There are some limitations in this study. Firstly, because images were acquired from different sensors, during the classification period, a different number of bands were used. Secondly, the training samples and classification results were only validated in 2009 due to lack of reference images.

In conclusion, Landsat images can be used to examine the LULC changes of the metropolitan area in long time series. The extent and spatial patterns of the GTA's urban expansion were both analyzed quantitatively and qualitatively in the study. It is feasible to integrate Landsat imagery and census data to study urban expansion of metropolitan areas or even of a global scale study over time. Since urban development policy making or urban planning usually need modeling of the urban growth tendency, knowing the urban historical development patterns and present developing situation are meaningful. Therefore, these results can be used for the regional governments or planners to make decisions regarding GTA's development in the future.

Acknowledgments

The authors would like to thank the USGS and Statistics Canada for providing valuable data sets used in this study. Thanks to the Geospatial Centre at the University of Waterloo for providing the reference images. The constructive comments and helpful suggestions from the anonymous reviewers are also acknowledged for improving the quality of the manuscript.

References

Abd El-Kawy, O.R., J.K. Rod, H. Ismail, and S. Suliman. 2011. Land use and land cover change detection in the western Nile delta of Egypt using remote sensing data. *Applied Geography*. *31*(2): 483–494.

Alphan, H., H. Doygun, and Y.I. Unlukaplan. 2009. Post-classification comparison of land cover using multitemporal Landsat and ASTER imagery: the case of Kahramanmaraş, Turkey. *Environmental Monitoring and Assessment*. 151: 327–336.

Bagan, H., and Y. Yamagata. 2012. Landsat analysis of urban growth: How Tokyo became the world's largest megacity during the last 40 years. *Remote Sensing of Environment*. 127: 210–222.

Bhatta, B. 2010. *Causes and Consequences of Urban Growth and Sprawl. In Analysis of Urban Growth and Sprawl from Remote Sensing Data*. Springer Berlin Heidelberg.

Burgess, W.E. 2008. The Growth of the City: An Introduction to a Research Project. *Urban Ecology*, 4: 16–26.

Congalton, R. 1991. A review of assessing the accuracy of classifications of remotely sensed data. *Remote Sensing of Environment*. 46: 35–46.

Congalton, R.G., and K. Green. 1999. *Assessing the Accuracy of Remotely Sensed Data: Principles and Practices*. ISBN 0-87371-986-7. CRC Press.

Conway, T.M. and J. Hackworth. 2007. Urban pattern and land cover variation in the Greater Toronto Area. *The Canadian Geographer*. 51(1): 43–57.

Dewan, A.M., and Y. Yamaguchi. 2009. Using remote sensing and GIS to detect and monitor land use and land cover change in Dhaka Metropolitan of Bangladesh during 1960–2005. *Environmental Monitoring and Assessment*. 150: 237–249.

DMTI CanMap Water. 2014. Markham, Ontario: DMTI Spatial Inc.

Elvidge, C.D., P.C. Sutton, and T.W. Wagner. 2004. *Urbanization. In Gutman, G., Janetos, A., Justice C., (eds.), Land Change Science: Observing, Monitoring, and Understanding Trajectories of Change on the Earth's Surface*. Dordrecht, Netherlands: Kluwer Academic Publishers.

Erbek, F.S., C. Özkan, and M. Taberner. 2004. Comparison of maximum likelihood classification method with supervised artificial neural network algorithms for land use activities. *International Journal of Remote Sensing*. *25*(9): 1733–1748.

Ferrato, L.J. and K.W. Forsythe. 2013. Comparing hyperspectral and multispectral imagery for land classification of the Lower Don River, Toronto. *Journal of Geography and Geology*. 5(1): 92–107

Forsythe, K.W. 2002. Stadtentwicklung in Calgary, Toronto, und Vancouver: Interpretation mit Landsatdaten. *In Proceedings of the 14th Symposium for Applied Geographic Information Processing*, 3–5.

Fu, A. 2014. *Urban Growth and LULC Change Dynamics Using Landsat Record of Region of Waterloo from 1984 to 2013*. Unpublished MSc Thesis, University of Waterloo.

Furberg, D., and Y. Ban. 2008. Satellite monitoring of urban sprawl and assessing the impact of land cover changes in the Greater Toronto Area. *ISPRS Archives*. 37(B7): 131–136.

Haregeweyn, N., G. Fikadu, A. Tsunekawa, M. Tsubo, and D.T. Meshesha. 2012. The dynamics of urban expansion and its impacts on land use/land cover change and small-scale farmers living near the

urban fringe: A case study of Bahir Dar, Ethiopia. *Landscape and urban planning*, *106*(2): 149–157.

Hu, H. and Y. Ban. 2008. Urban land-cover mapping and change detection with RADARSAT data using neural network and rule-based classifier., *ISPRS Archives*. 37(B7): 1549–1554.

Huang, C., L.S. Davis, and J. R.G. Townshend. 2002. An assessment of support vector machines for land cover classification. *International Journal of Remote Sensing*. 23(4): 725–749.

Lackner, M., and T.M. Conway. 2008. Determining land-use information from land cover through an object-oriented classification of IKONOS imagery. *Canadian Journal of Remote Sensing*. 34(2):77–92.

Ma, Y. and R. Xu. 2010. Remote sensing monitoring and driving force analysis of urban expansion in Guangzhou City, China. *Habitat International*. 34: 228–235.

Martin, L.R., and P.J. Howarth. 1989. Change-detection accuracy assessment using SPOT multispectral imagery of the rural-urban fringe. *Remote Sensing of Environment*. 30(1): 55–66.

Manandhar, R., I.O. Odeh, and T. Ancev. 2009. Improving the accuracy of land use and land cover classification of Landsat data using post-classification enhancement. *Remote Sensing*. 1(3): 330–344.

Otukei, J.R., and T. Blaschke. 2010. Land cover change assessment using decision trees, support vector machines and maximum likelihood classification algorithms. *International Journal of Applied Earth Observation and Geoinformation*. 12: S27–S31.

Peiman, R. 2011. Pre-classification and post-classification change-detection techniques to monitor land-cover and land-use change using multi-temporal Landsat imagery: a case study on Pisa Province in Italy. *International Journal of Remote Sensing*. *32*(15): 4365–4381.

Schmidt, K.S., and A.K. Skidmore. 2003. Spectral discrimination of vegetation types in a coastal wetland. *Remote Sensing of Environment*. 85: 92–108.

Schneider, A. 2012. Monitoring land cover change in urban and peri-urban areas using dense time stacks of Landsat satellite data and a data mining approach. *Remote Sensing of Environment*. 124: 689–704.

Silván-Cárdenas, J.L., L. Wang, P. Rogerson, C. Wu, T. Feng, and B.D. Kamphaus. 2010. Assessing fine-spatial-resolution remote sensing for small-area population estimation. *International Journal of Remote Sensing*. 31(21): 5605–5634.

Singh, A. 1989. Digital change detection techniques using remotely sensed data, *International Journal of Remote Sensing*. 10: 989–1003.

Squires, G.D. 2002. *Urban Sprawl and the Uneven Development of Metropolitan America. In Squires, G.D. (ed.), Urban Sprawl: Causes, Consequences, and Policy Responses*. Washington, D.C. Urban Institute Press.

Stan, A.I. 2013. Morphological Patterns of Urban Sprawl Territories. *Urbanism. Arhitectură. Constructii*. 4(4): 11–24.

Statistics Canada. 2011. Retrieved from: http://www12.statcan.gc.ca/census-recensement/index-eng.cfm?MM

Sundarakumar, K., M. Harika, S.K.A. Begum, S. Yamini, and K. Balakrishna. 2012. Land use and land cover change detection and urban sprawl analysis of Vijayamada city using multitemporal Landsat data. *International Journal of Engineering Science and Technology*. 4(01): 170–178.

Tan, K.C., H.S. Lim, M.Z. MatJafri and K. Abdullah. 2010. Landsat data to evaluate urban expansion and determine land use/land cover changes in Penang Island, Malaysia. *Environmental Earth Sciences*. *60*: 1509–1521.

Tole, L. 2008. Changes in the built vs. non-built environment in a rapidly urbanizing region: a case study of the Greater Toronto Area. *Computers, Environment and Urban Systems*. 32(5): 355–364.

Wacker, A.G., and D.A. Landgrebe. 1972. The minimum distance approach in remote sensing, *LARS Technical Reports*. Purdue University.

Yang, X, 2011. Parameterizing support vector machines for land cover classification. *Photogrammetric Engineering & Remote Sensing*. 77(1): 27–37.

Yuan, F., K.E. Sawaya, B.C. Loeffelholz, and M.E. Bauer. 2005. Land cover classification and change analysis of the Twin Cities (Minnesota) Metropolitan Area by multitemporal Landsat remote sensing. *Remote Sensing of Environment*. 98(2): 317–328.

Yuan, D., C.D. Elvidge, and R.S. Lunetta. 1998. Survey of multispectral methods for land cover change analysis. *Remote Sensing Change Detection: Environmental Monitoring Methods and Applications*. Chelsea, Michigan: Ann Arbor. 21–39.

Zhao, H., and J. Li. 2005. Urban change detection and population prediction modeling using remotely sensed images. *Geomatica*. 59(2): 49–59.

Authors

Lanying Wang is a candidate for a Master of Science from the Department of Geography and Environmental Management, University of Waterloo, and a research associate of the Geo-STARS Laboratory. She received a BSc degree in geomatics from Tianjin Normal University, China, in 2011. Her research interests include remote sensing image processing, and laser scanning data processing. Her current research focuses on using mobile laser scanning data to generate high accuracy digital terrain models.

Wei Li is a graduate student of the University of Waterloo since August 2013. She is also a

research fellow of the Geospatial Technology and Remote Sensing Lab at the Department of Geography and Environmental Management, University of Waterloo. She completed a Bachelor's degree of Marine Science in China University of Geosciences (Beijing) in 2012. Her research interests include remote sensing image processing, urban change detection, building extraction by high resolution images, and human geography. She has co-authored several published conference papers.

Shiqian Wang is a master student in University of Waterloo. She received an undergraduate degree in Wuhan University, China, in 2012. Her current research interests include remote sensing image processing and mobile laser scanning data analysis.

Jonathan Li received his PhD degree in photogrammetry and remote sensing from the University of Cape Town, South Africa. He is currently a Professor with the Department of Geography and Environmental Management, University of Waterloo, Canada, and heads the GeoSTARS Laboratory. He has published over 300 papers in refereed journals, books and proceedings, more than 50 of which were published in top-ranked remote sensing journals, such as RSE, TGRS, ISPRS, TITS, IJRS, GRSL, J-STARS, PE&RS, JAG. His current research interests include urban remote sensing, mobile laser scanning point cloud processing, feature extraction and 3D surface modeling. Dr. Li is Chair of ISPRS ICWG I/Va on Mobile Scanning and Imaging Systems (2012–2016), Vice Chair of ICA Commission on Mapping from Remote Sensor Imagery (2011–2015), Vice Chair of FIG Commission IV on Hydrography and the Chair of FIG WG4.4 on Maritime and Marine Spatial Information Management (2015–2018). He has been Associate Editor of *Geomatica* in remote sensing since 2007. ❑